Ab initio study of electronic properties in free and matrix-isolated iron dihalides

E. L. Bominaar, J. Guillin, A. Sawaryn, and A. X. Trautwein
Institut für Physik, Medizinische Universität, D-2400 Lübeck, Federal Republic of Germany
(Received 2 May 1988)

Ab initio Hartree-Fock calculations are performed in the molecular $^5\Delta_g$, $^5\Pi_g$, and $^5\Sigma_g^+$ states of the dihalides $FeCl_2$ and $FeBr_2$ at experimental and geometry-optimized atomic separations. Molecular-term energies, ionization energies, bond energies, electric-field gradients (EFG), and electron densities $\rho(o)$ (the latter two quantities at the iron nucleus) are evaluated and compared with experiment. Electron-correlation corrections and basis-set effects on the energies, EFG, and $\rho(0)$ are studied. The relative isomer shift of noble-gas-matrix-isolated $FeCl_2$ and Fe^0 is analyzed on the basis of electron densities calculated in $FeCl_2$–noble-gas and Fe^0–noble-gas clusters.

INTRODUCTION

The combined effort in experimental and theoretical research during the last three decades has greatly improved the understanding of the electronic structure of transition-metal complexes. Much interest has been devoted to transition-metal dihalides, and especially for the two iron-containing compounds $FeCl_2$ and $FeBr_2$, detailed experimental data are available. Among the various authors, unanimity is found concerning the molecular geometry and ground states of the two dihalides. However, the theoretical interpretations of the Mössbauer-effect data of noble-gas-matrix-isolated (NGMI) dihalides, presented in the literature, are mutually contradictory. Notably, the quadrupole splittings of $FeCl_2$ and $FeBr_2$,[1,2] for which only the absolute values are available, have been reproduced from calculated electric-field gradients (EFG's) of both signs.[3,4]

In view of the linearity established in a number of other metal dihalides[5] and the fact that infrared spectra,[6] electronic absorption spectra,[5] charge-transfer spectra,[7] and photoelectron spectra[8] in $FeCl_2$ and $FeBr_2$ are satisfactorily interpreted on this basis, these molecules are generally considered to be linear. There seems to exist only some discrepancy between bending frequencies deduced from temperature-dependent shrinkage of linear $FeCl_2$ observed in the electron-diffraction study of Vajda *et al.*[9] and obtained from infrared-spectroscopy studies of the molecule either in noble-gas matrix[10] or in gas phase.[6]

DeKock and Gruen[5] adopting an intermediate axial crystal-field description in the analysis of electronic absorption spectra in gaseous MCl_2, M=V–Cu transition metals, concluded a high-spin $^5\Delta_g$ ground state in $FeCl_2$ and assigned lines observed for this molecule at 4600 and 7140 cm^{-1} to Laporte forbidden $^5\Delta_g$-$^5\Pi_g$ and $^5\Sigma_g^+$-$^5\Pi_g$ transitions, respectively. In the study by the same authors of charge-transfer spectra in the matrix-isolated molecules[7] MCl_2, M=Mn–Ni transition metals, the $^5\Delta_g$ ground state in $FeCl_2$ is confirmed by comparing observed and predicted spectral-line numbers. Since all molecular states considered here are of gerade symmetry we shall further drop the subscript g from the notation.

In the combined experimental and theoretical study of Berkowitz *et al.*[8] on gas-phase photoelectron spectra of the transition-metal dihalides MX_2, M=Mn–Ni transition metals, X=Cl,Br, the experimental ionization energies are compared with one-electron molecular-orbital (MO) energies in the transition state obtained from spin-restricted and spin-unrestricted multiple-scattering cellular $X\alpha$ calculations. The spin-unrestricted scheme leads again to $^5\Delta$ ground states in $FeCl_2$ and $FeBr_2$, and the significantly lower first-ionization potentials measured in the Fe and Co dihalides, relative to those of the other members in the series, correlate satisfactorily with the behavior of the MO energies of the $d_\delta^\downarrow$ ($\downarrow$ minority spin) electron.

The Hartree-Fock-Slater (HFS) $X\alpha$ calculations in $FeCl_2$ and $FeBr_2$ by Ellis *et al.*[3] confirm once more the $^5\Delta$ ground state in the two dihalides and the $d_\delta^\downarrow$ character of the weakest-bonded electron. The electric-field gradients presented by the same authors, show a strong variation with the iron-halogen distance and are furthermore sensitively dependent on the definition of the electronic model potentials in their method. The most sophisticated calculational scheme leads thereby, in the two dihalides, to negative EFG's with quadrupole splittings of magnitudes in reasonable agreement with experiment.

By combining EFG's from unrestricted Hartree-Fock (UHF) calculations and experimental quadrupole splittings in $FeCl_2$ and $FeBr_2$, Duff *et al.*[4] deduced a nuclear quadrupole moment Q for ^{57}Fe of about half the value 0.15 b (Ref. 11) adopted here. In their analysis, the largest contributions to the EFG originate from the Fe $3d$ shell and the halogen atoms. However, mutual cancellation leads to a total EFG of an order of magnitude smaller than the separate contributions, which makes the EFG sensitively dependent on Fe $3p$-electron contributions.

Since Mössbauer studies on $FeCl_2$ and $FeBr_2$ are performed on matrix-isolated molecules, it is of interest to study the effect of the matrix atoms on the Mössbauer parameters. The theoretical matrix-effect studies which have appeared up to now mainly deal with NGMI iron; for molecular systems like $FeCl_2$ such investigations are

lacking. A number of arguments can be produced against or in favor of the importance of the noble-gas effect on matrix-isolated molecules.[4] (1) The small shifts in asymmetric-stretching frequencies between NGMI and gas-phase dihalides indicate, for this property, a small noble-gas effect.[6,10] (2) The equal values of the quadrupole splittings, ΔE_Q, and/or isomer shifts, δ, observed in NGMI $FeCl_2$ (Ref. 1) and in NGMI Fe (Refs. 12 and 13) for different noble-gas matrices can be explained[4] by assuming negligible noble-gas interactions. (3) On the other hand, calculations in Fe-noble-gas clusters result in non-negligible matrix effects[14–16] which, under certain plausible conditions, become equal for different hosts.[15] (4) The small quadrupole splitting, $\Delta E_Q \approx 0.6$ mm s^{-1}, of NGMI $FeCl_2$, compared with the value of 2 mm s^{-1} for $FeCl_2$ deposited on graphite, observed in Mössbauer studies of Shechter *et al.*[17] is interpreted by these authors as an indication for strong $FeCl_2$–noble-gas interactions.

In this paper we study the electronic structure of the molecules $FeCl_2$ and $FeBr_2$ by quantum-chemical *ab initio* methods. Linear geometry in the two dihalides is adopted in all calculations. Geometry optimizations are carried out for various electronic configurations, using different basis sets. Molecular-term energies, ionization energies, bond energies, electric-field gradients, and electron densities are calculated. The geometry, basis-set, and electron-correlation dependences of the energies, quadrupole splittings, and isomer shifts are discussed. Finally, the isomer shift of NGMI $FeCl_2$ relative to NGMI Fe^0 is analyzed on the basis of electron densities at the iron nucleus calculated in $FeCl_2$–noble-gas and Fe^0–noble-gas clusters.

METHOD AND BASIS SET

The all-electron calculations presented here are performed with the GAUSSIAN86 quantum-chemical *ab initio* program.[18] The various molecular states of $FeCl_2$ and $FeBr_2$ are constructed by applying the unrestricted Hartree-Fock procedure[19] to a suitable guess wave function of required spin and orbital symmetry. The UHF calculations at the experimental separations are supplemented with geometry optimization in linear conformation. In each calculation, the EFG and the electronic charge density at the iron nucleus, $\rho(0)$, are evaluated. In order to estimate the contributions of electron correlation to the energies, EFG, and $\rho(0)$, corrections up to fourth-order Møller-Plesset perturbation theory (MP4) (Ref. 20) are calculated in $FeCl_2$.

Since the *s* electrons in iron are subjected to considerable relativistic effects, which are not taken into account in the UHF procedure adopted here, the nonrelativistic $\rho(0)$ values are scaled by a relativistic correction factor *S* (Ref. 21) resulting from the interpolation formula $S = a + b(n_s - 6) + c(n_d - 6)$. In this expression, n_s and n_d represent the numbers of Fe *s* and Fe *d* electrons as defined in Mulliken population analysis, and *a*, *b*, and *c* coefficients with values 1.388 8898, -1.23×10^{-5}, and 1.636×10^{-4}, respectively.[21] We note that the calibration constant α' obtained by combining experimental isomer shifts and nonrelativistic charge densities, $\delta = \alpha' \Delta\rho_{\text{nonrel}}(0)$, is generally larger by a factor of about 1.4 than the relativistic value $\alpha = -0.23$ mm s^{-1} a_0^3 (Refs. 22 and 23) used here.

In a previous theoretical study on free and NGMI Fe*X*, *X*=H, C, N, and O, we observed various degrees of basis-set dependence in the results for geometry optimization, molecular ground state and Mössbauer parameters.[15,24] Therefore, we investigate, also in this paper, the influence of different basis sets on our results. Three of the basis sets applied here (Table I) are constructed by splitting and extension of a basis set given by Huzinaga *et al.*[25] Moreover, standard STO-3G and STO-3G* bases are used, and we note that the basis set III for iron and neon (see Table I) is taken from Refs. 15 and 24.

RESULTS AND DISCUSSION

Free iron dihalides

In Table II we present the results of our calculations in $FeCl_2$ and $FeBr_2$ for optimized geometries, relative energies of the various configurations considered, bond energies, and Mössbauer parameters, i.e., quadrupole splitting ΔE_Q and relative isomer shift $\Delta\delta$. The quadrupole splitting is obtained from the value for the main component, *q*, of the EFG tensor, using the relation $\Delta E_Q = \frac{1}{2} e^2 q Q$ and taking for the nuclear quadrupole moment $Q(^{57}\text{Fe})$ the value 0.15 b.[11] In case of the $^5\Pi$ state, where the main component of the EFG is perpendicular to the molecular axis, the values between parentheses in the table correspond to the component of the EFG along the molecular axis.

TABLE I. Definitions of the basis sets and contraction patterns of I–III derived from Huzinaga standard bases (Ref. 25).

Basis	Fe	Cl	Br	Ne	Ar
I	5333/521/5	533/53	4333/433/4	53/5	533/53
II	5333/531[a]1[b]/5	533/53	4333/433/4	53/5	533/53
III	532 111[c]/53 311/411[d]	5321/521	4333/433/4	521/41	5321/521
IV	STO-3G for all atoms				
V	STO-3G* for all atoms				

[a]Primitive Gaussian, $\exp(-\beta r^2)$, with orbital exponential factor $\beta = 0.25 a_0^{-2}$.
[b]$\beta = 0.10 a_0^{-2}$.
[c]Primitive Gaussian with $\beta = 0.844\,766\,3 a_0^{-2}$ is skipped from the Huzinaga basis.
[d]$\beta = 0.14 a_0^{-2}$.

TABLE II. UHF and MP4 results for free iron dihalides and free neutral iron, i.e., optimized (O) distances (R), relative total energies (E_{rel}), bond energies (E_{bond}), quadrupole splittings (ΔE_Q), asymmetry parameters (η), and isomer shifts ($\Delta\delta$) relative to free and NGMI Fe^0.

Molecule and config.	Basis	Type of calc.	R (Å)	E_{rel} (mhartree)	E_{bond}[a] (hartree)	ΔE_Q[b] (mm s^{-1})	η	$\Delta\delta$ (mm s^{-1})[c] Rel. free Fe^0	Rel. NGMI Fe^0
					$FeCl_2$				
$^5\Delta$	I	UHF/O	2.237	0	0.12	+0.58	0.0	+1.10	+1.50
		UHF	2.160	3		+0.05	0.0		
$^5\Pi$		UHF/O	2.255	12		+5.16	0.9	+1.05	+1.45
						(−4.82)			
$^5\Sigma^+$		UHF/O	2.242	14		−6.73	0.0	+0.95	+1.35
$^3\Delta$		UHF/O	2.267	191		−10.2	0.0	+1.04	+1.44
$^5\Delta$	II	UHF/O	2.264	0	0.19	+0.88	0.0	+1.18	+1.58
		MP4	2.264	0		+0.83	0.0	+1.06	+1.46
		UHF	2.160	6		+0.37	0.0	+1.10	+1.50
		MP4	2.160	5		+0.33	0.0	+0.98	+1.38
		MP4/O	2.261	0		+0.85	0.0	+1.06	+1.46
$^5\Pi$		UHF/O	2.272	11		+5.29	0.8	+1.14	+1.54
						(−4.83)			
		MP4	2.272	11		+5.29	0.8	+1.02	+1.42
						(−4.86)			
$^5\Sigma^+$		UHF/O	2.260	13		−6.75	0.0	+1.03	+1.43
		MP4	2.260	8		−6.72	0.0	+0.90	+1.30
$^5\Delta$	III	UHF/O	2.244	0	0.22	+0.40	0.0	+1.20	+1.60
		UHF	2.160	4		+0.01	0.0	+1.11	+1.51
		MP4	2.244	0		+0.15	0.0	+1.11	+1.51
$^5\Pi$		UHF/O	2.255	17		+4.80	0.9	+1.14	+1.54
						(−4.54)			
		MP4	2.255	20				+1.05	+1.45
$^5\Sigma^+$		UHF/O	2.231	17		−6.07	0.0	+0.85	+1.25
$^5\Delta$	IV	UHF/O	2.124	0	0.31	+2.71	0.0		
$^5\Pi$		UHF/O	2.119	−11		+2.31	0.1		
						(−1.21)			
$^5\Sigma^+$		UHF/O	2.147	−189		−1.43	0.0		
$^5\Delta$	V	UHF/O	2.107	0	0.29	+0.73	0.0		
$^5\Pi$		UHF/O	2.114	17		+2.39	0.7		
						(−2.03)			
$^5\Sigma^+$		UHF/O	2.066	−4		−2.76	0.0		
Expt.			2.160		0.15	+0.63			+1.63[d]

Using basis sets I–III the $^5\Delta$ is found as the ground state; with STO-3G and STO-3G* (basis sets IV and V) $^5\Sigma^+$ is lowest in energy. Therefore, in view of the strong evidence in favor of the $^5\Delta$ ground state discussed in the Introduction, the STO-3G and STO-3G* basis sets seem to be less appropriate for the description of the electronic structure in the two dihalides. In addition, the bond energies, obtained with basis sets IV and V are about twice the experimental values, while with basis sets I–III better agreement is found with experiment. On the other hand, the optimized distances obtained with the STO-3G and STO-3G* basis sets of 0.05 Å below the experimental distance are in better agreement with experiment than the values found using I–III. The spin-triplet configuration considered in $FeCl_2$ is 0.2 hartree above the $^5\Delta$ level. The energy separations between the $^5\Delta$, $^5\Pi$, and $^5\Sigma^+$ levels, obtained with the basis sets I–III, are about half the experimental values reported by DeKock *et al.*[5]

In Table III we present ionization energies of $FeCl_2$, calculated with basis set III at the optimized distance 2.244 Å, from subtraction of the total UHF-state energies of the ground state $^5\Delta$ and the configurations obtained after removal of the electrons indicated. The arrows ↑ and ↓ indicate one-electron spins, respectively, parallel and antiparallel to the total spin. Furthermore, the ionization potentials obtained from one-electron MO energies,[26] ϵ, calculated in the ground state $^5\Delta$ with basis set III and from the transition-state energy eigenvalues[27] presented in Refs. 3 and 8 are given in the table. The energies of the molecular orbitals of mainly $d^\uparrow$ character are about −20 eV and lie about 7 eV in energy below the 12 highest occupied ligand $p(\pi,\sigma)$ orbitals in the two dihalides. The relaxation, occurring after electron removal, lowers the ionization energies of the ligand p electrons obtained from the total-energy subtractions, uniformly by 0.5 eV relative to the MO energies. The most remarkable feature in Table III is the lowest ionization energy found for the $d^\downarrow_\delta$ electron in the total-energy cal-

TABLE II. (*Continued*).

Molecule and config.	Basis	Type of calc.	R (Å)	E_{rel} (mhartree)	E_{bond}[a] (hartree)	ΔE_Q[b] (mm s^{-1})	η	$\Delta\delta$ (mm s^{-1})[c] Rel. free Fe^0	Rel. NGMI Fe^0
					$FeBr_2$				
$^5\Delta$	I	UHF/*O*	2.412	0	0.10	+1.20	0.0	+1.08	+1.48
		UHF	2.310	4		+0.62	0.0		
$^5\Pi$		UHF/*O*	2.423	8		+4.89	0.7	+1.03	+1.43
						(−4.26)			
$^5\Delta$	II	UHF/*O*	2.425	0	0.17	+1.15	0.0	+1.16	+1.56
		UHF	2.310	6		+0.67	0.0	+1.09	+1.49
$^5\Pi$		UHF/*O*	2.426	8		+5.17	0.8	+1.12	+1.52
						(−4.58)			
$^5\Delta$	IV	UHF/*O*	2.253	0	0.28	+2.64	0.0		
$^5\Pi$		UHF/*O*	2.244	−12		+2.37	0.1		
						(−1.28)			
$^5\Sigma^+$		UHF/*O*	2.278	−189		−1.39	0.0		
Expt.			2.31		0.13	+0.86			+1.56[d]
					Fe^0				
$^5\Sigma^+$	I	UHF				−3.75	0.0		
	II	UHF				−3.91	0.0		
	III	UHF				−3.34	0.0		

[a] $E_{bond} = E(FeX_2) - E(Fe) - 2E(X)$; X=Cl,Br. Experimental values are taken from Ref. 8.
[b] Value in parentheses corresponds to EFG along z direction, see text.
[c] $\Delta\delta$ derived from calculated $\Delta\rho(0)$ using $\Delta\delta = -0.23$ mm s^{-1} $a_0^3\,\Delta\rho(0)$.
[d] Value obtained from combining experimental isomer shift of NGMI $FeCl_2$ (Br_2) relative to α-Fe (Refs. 1 and 2) and experimental isomer shift of NGMI Fe^0 relative to α-Fe (Ref. 12).

TABLE III. Comparison of experimental one-electron ionization energies (eV) of $FeCl_2$ and orbital energies obtained from transition-state calculations by Berkowitz *et al.* (Ref. 8) and Ellis *et al.* (Ref. 3) and by subtraction of UHF ground- and ionized-configuration energies in the present work, using basis set III and Fe—Cl distance 2.244 Å. The arrows ↑ and ↓ indicate one-electron spins parallel and antiparallel to the total spin. ϵ are, for the orbital symmetries indicated, the highest occupied one-electron orbital energies in the $^5\Delta$ ground configuration.

Total-energy calculations		$-\epsilon$	One-electron ionization energies (eV) Ref. 8	Ref. 3	Expt.[a]
Fe 3*d* character	$\delta_g^\downarrow$ 11.0(10.8)[b]	15.1	$\delta_g^\downarrow$ 9.3	$\delta_g^\downarrow$ 9.4	10.45
Mainly	$\pi_g^\uparrow$ 11.6	12.1	$\sigma_g^\uparrow$ 10.8	$\pi_g^\uparrow$ 10.0	11.26
ligand	$\pi_u^\downarrow$ 11.8	12.3	$\pi_g^\uparrow$ 10.8	$\pi_u^\downarrow$ 10.3	11.91
character	$\pi_g^\downarrow$ 11.9	12.4	$\pi_u^\downarrow$ 11.4	$\sigma_u^\uparrow$ 11.3	12.12
	$\pi_u^\uparrow$ 12.0	12.4	$\pi_u^\uparrow$ 11.5	$\delta_g^\uparrow$ 11.7	12.53
	$\sigma_u^\uparrow$ 12.2	12.8	$\pi_g^\downarrow$ 11.8	$\sigma_g^\uparrow$ 11.9	13.67
	$\sigma_u^\downarrow$ 12.3	12.9	$\sigma_u^\downarrow$ 12.1		
	$\sigma_g^\uparrow$ 13.0	13.4	$\sigma_u^\uparrow$ 12.5		
	$\sigma_g^\downarrow$ 13.6	14.0	$\delta_g^\uparrow$ 13.0		
Fe 3*d* character	$\delta_g^\uparrow$ 15.8	19.3	$\pi_g^\uparrow$ 13.5		
			$\sigma_g^\downarrow$ 13.8		

[a] Berkowitz *et al.* (Ref. 8).
[b] Value in brackets corresponds to energy difference of UHF energies obtained after geometry optimization in ground *and* ionized configurations.

culations, in agreement with the transition-state energy eigenvalues[3,8] but in disagreement with the one-electron ionization energy $-\epsilon$. The large difference between the total-energy and the one-electron-energy results for the $3d_\delta$ electrons indicate a considerable relaxation after ionization. Our calculated ionization energy for the $d_\delta^\downarrow$ electron is about 0.5 eV above the experimental value, given in Table III, while the results of Berkowitz *et al.*[8] and Ellis *et al.*[3] are about 1 eV too low. We note that additional geometry optimizations in the ionized states reduce the gap between the calculated and experimental ionization energies. For the $d_\delta^\downarrow$ electron we thus find the ionization energy 10.8 eV, in reasonable agreement with the experimental value 10.45 eV.[8]

The isomer shifts presented in Table II are relatively insensitive with respect to molecular state, basis set, distances, and correlation effects. The experimental isomer shifts of 1.63 and 1.56 mm s^{-1}, for $FeCl_2$ (Refs. 1 and 2) and $FeBr_2$ (Ref. 2), respectively, relative to NGMI Fe^0 are around 1.5 times larger than the calculated values. In the discussion below, we shall show that this discrepancy can be partially attributed to the effect of the noble-gas matrix on Fe^0.

The quadrupole splittings of $^5\Delta$ in Table II show for each basis set a decrease when the atomic separations are reduced. Similar qualitative behavior of the quadrupole splitting with distance is found by Ellis *et al.*,[3] but, in contrast to their results, our values for ΔE_Q in the ground state remain positive at the experimental geometry. The values of the quadrupole splittings at the optimized geometries for basis sets I–III are larger than at the experimental distances, and it depends on the basis set for which, of the two separations, the best result is obtained. The basis-set dependence of the calculated quadrupole splittings indicates that the basis sets adopted here are not "saturated" in the determination of the EFG. The effect of electron correlation on ΔE_Q is small in magnitude (0.25 mm s^{-1} for basis set III), in agreement with our earlier studies on iron carbonyls,[21,24] but considerable on a relative scale (60% of ΔE_Q at the optimized geometry for $^5\Delta$ with basis set III).

Concerning the effect of spin-orbit coupling on the EFG in iron dihalides, we note that, in first-order perturbation theory, the $^5\Delta$ term of ferrous iron, arising in the axial ligand field of the two halide atoms, is split into five doublets, with an equidistant term scheme of separation equal to half the one-electron spin-orbit coupling constant, without changing the EFG. The lowest level, which is thermally almost uniquely occupied in NGMI experiments, corresponds to a pure total-angular momentum $J=4$ state of ferrous iron, having no second- or higher-order admixture with iron $^5\Pi$ and $^5\Sigma^+$ configurations. Consequently, we do not expect any substantial change of the EFG in the ground state due to spin-orbit coupling.

The small value of the quadrupole splitting in the ground state of the two dihalides makes this quantity more susceptible to contributions which are only of minor importance in molecules with large ΔE_Q values. For this reason, NGMI $FeCl_2$ and NGMI $FeBr_2$ are less appropriate for the determination of the nuclear quadrupole moment, $Q(^{57}Fe)$, from calculated EFG and experimental ΔE_Q values.[4] Such a procedure becomes more reliable when various compounds with large EFG of different sign are considered.[23,28] It seems that, up to the present date, the physical data of various disciplines cannot be interpreted on the basis of a common value of Q. The small Q value, 0.082 b, given by Duff *et al.*[4] is supported, for instance, by nuclear shell model calculations on ^{54}Fe in combination with the measured ratio $Q(^{57}Fe)/Q(^{54}Fe)$.[29] On the other hand, if one adopts this small Q value, it is impossible to explain the very large ΔE_Q values, larger than 4 mm s^{-1}, found in pentacoordinated iron(II) "picket fence" porphyrins, because the EFG mainly originates in this case from one electron in a nonbonding Fe $3d_{xy}$ orbital.[30,31]

Noble-gas-matrix effects

In Fig. 1 we plot the difference between the electron density at the iron nucleus of NGMI Fe^0 and free Fe^0, $\Delta\rho(0)$, obtained in UHF calculations with basis set III in various iron–noble-gas clusters, as a function of the iron–noble-gas atom distance. The charge density reaches a maximum at a Fe^0-Ne(Ar) separation lying between the nearest-neighbor distance in the neon (argon) lattice 3.2 Å (3.8 Å) and the extended x-ray-absorption fine-structure (EXAFS) value for Fe^0-Ne (Ar) 2.45 Å (2.82 Å) reported by Purdum *et al.*[32] and Montano *et al.*,[33] respectively. We also find that, at a fixed iron-neon distance, the value $\Delta\rho(0)$ is an almost linear function of the number of neighboring noble-gas atoms, independent of the geometrical details of the clusters (Fig. 2). Furthermore, the results presented in Figs. 1 and 2 are independent of the $^5\Delta$, $^5\Pi$, and $^5\Sigma^+$ configurations of the iron atom, used in the calculations. The UHF calculations in the cluster with 12 neon atoms, at 3.2 Å from Fe,

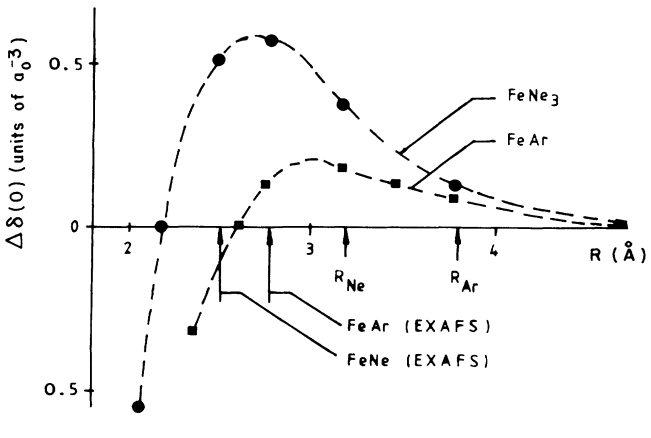

FIG. 1. Dependence of $\Delta\rho(0)$ on the internuclear distance between iron and noble-gas atoms. The quantity $\Delta\rho(0)$ represents the difference between electron densities $\rho_{\text{cluster}}(0)$ and $\rho_{\text{free iron}}(0)$. R_{Ne} and R_{Ar} correspond to nearest-neighbor distances between noble-gas atoms in solid neon and argon, respectively. EXAFS studies of Fe^0 in neon yield an Fe-Ne distance 2.45 Å (Ref. 32) and of Fe^0 in argon two Fe-Ar distances, 2.82 and 3.72 Å, respectively.[33]

TABLE IV. Total Mulliken populations of s, p, and d shells of iron in $FeCl_2$ and $FeBr_2$, calculated in the UHF ground state $^5\Delta$, at optimized geometry for basis set I, II, and III, respectively.

	Basis	s	p	d
$FeCl_2$	I	6.4	12.0	6.1
	II	6.4	12.5	6.1
	III	6.4	12.4	6.3
$FeBr_2$	I	6.5	12.0	6.1
	II	6.5	12.6	6.0

representing the nearest-neighbor cluster of iron substituted at a site in solid neon, yields $\Delta\rho(0)=1.64a_0^{-3}$. A linear extrapolation of the $\Delta\rho(0)$ results, obtained for small clusters, to larger clusters gives for Fe^0-Ne_{12} (Fe-Ne distance is 2.45 Å) and Fe^0-Ar_{12} (Fe-Ar distance is 2.82 Å and 3.8 Å) the values $\Delta\rho(0)=2.13a_0^{-3}$ and $\Delta\rho(0)=1.80a_0^{-3}$ and $1.60a_0^{-3}$, respectively. Our extrapolated *ab initio* $\Delta\rho(0)$ value for Fe^0-Ar_{12} is in agreement with the value $1.77a_0^{-3}$ of Braga *et al.*[14] calculated by the multiple-scattering $X\alpha$ method in a Fe^0-Ar_{12} cluster (Fe-Ar distance is 3.8 Å). Consequently, NGMI Fe^0 acquires a negative isomer shift of approximately -0.4 mm s^{-1} relative to *free* Fe^0. The addition of this matrix effect leads to recalculated isomer shifts for $FeCl_2$ and $FeBr_2$ relative to NGMI Fe^0, which considerably reduces the gap between calculated and experimental isomer shifts (Table II). Another interesting feature displayed in Fig. 2 is the decrease of the noble-gas-matrix effect on the electronic charge density at the iron nucleus in the series Fe^0 $4s^2$, Fe^+ $4s^1$, and Fe^{2+} $4s^0$, proportional to the iron $4s$-orbital occupation, at fixed iron–noble-gas distance. The importance of the $4s$ electrons in the description of the matrix effect on $\Delta\rho(0)$ is in all probability related to the

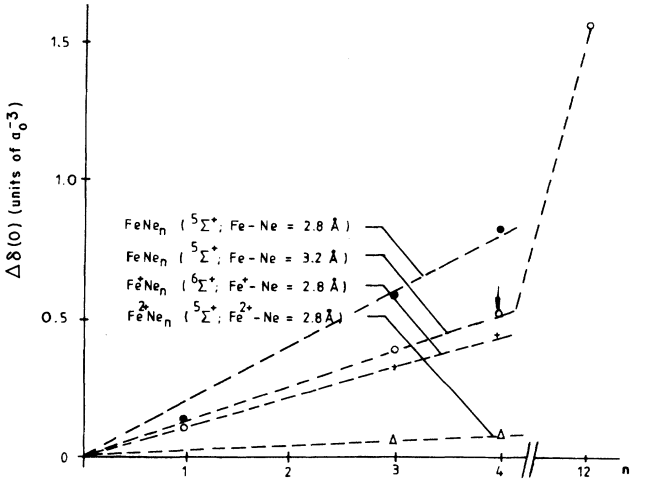

FIG. 2. Dependence of $\Delta\rho(0)$ for Fe, Fe^+, and Fe^{2+} on the number of noble-gas neighbors in clusters consisting of iron equidistantly surrounded by noble-gas atoms. The value indicated by an arrow is obtained for iron in a square-planar and in a tetragonal environment of four neon atoms.

large radial extension of the iron $4s$ orbitals. Since the iron $4s$-orbital occupation of the two dihalides, given in Table IV, is about 0.5 electrons only, the matrix effect on these molecules is expected to be significantly smaller than on Fe^0.

In order to study the noble-gas effect on the Mössbauer parameters in the $^5\Delta$ ground state of NGMI $FeCl_2$, a number of UHF calculations in small $FeCl_2 \cdots n$Ne clusters, $n=2,\ldots,6$ are performed, the results of which are summarized in Table V. The calculations for basis set I are made at a fixed Fe—Cl distance of 2.25 Å; for basis sets II and III the optimized separations of the free $FeCl_2$ molecule (see Table II) are taken. Since no structural

TABLE V. Calculated quadrupole splitting (ΔE_Q) and isomer shift ($\Delta\delta$) for NGMI $FeCl_2$; $\Delta\delta$ is relative to free $FeCl_2$.

Basis	Model structure of NGMI $FeCl_2$[a]	ΔE_Q (mm s^{-1})	$\Delta\delta$ (mm s^{-1})[c]
I	(0,±2.45,0)	+0.66	+0.04
	(0,0,±4.7)	+0.62	−0.02
	free $FeCl_2$	+0.67	0
II	(0,±2.45,0)	−1.20(+0.67)[b]	+0.03
	free $FeCl_2$	+0.88	0
III	(0,±2.45,0)	−0.86(+0.24)[b]	+0.03
	(0,0,±4.5)	+0.26	−0.05
	(0,0,±4.694)	+0.32	−0.03
	(0,0,±5.444)	+0.39	−0.00
	(±2.45,0,0)(0,±2.45,0)	+0.34	+0.06
	(±3.2,0,0)(0,±3.2,0)	+0.38	+0.00
	(±2.26,0,2.244)(0,±2.26,2.244)	+0.35	−0.03
	(±3.2,0,0)(0,±3.2,0)(0,0,±4.5)	+0.23	−0.05
	free $FeCl_2$	+0.40	0

[a]Fe is at origin; coordinates of Cl are $(0,0,\pm R)$, with $R=2.25$, 2.264, and 2.244 for basis I, II, and III, respectively; coordinates in parentheses refer to Ne; all distances in Å.

[b]Value in parentheses corresponds to EFG along z direction; see text.

[c]$\Delta\delta$ derived from calculated $\Delta\rho(0)$ using $\Delta\delta=-0.23$ mm s^{-1} $a_0^3\Delta\rho(0)$.

data are available for the positions of the noble-gas atoms around NGMI $FeCl_2$, we consider various structures, viz., "linear" structures with Ne atoms along the molecular axis, "perpendicular" structures with the Ne atoms in a plane through Fe or Cl perpendicular to the molecular axis, and a combination of the two possibilities. The Ne-Fe(Cl) distance of 2.45 Å is equal to the Fe-Ne distance reported by Purdum *et al.*[32] for NGMI Fe^0. The results in Table V for the isomer shift of NGMI $FeCl_2$ relative to free $FeCl_2$, $\Delta\delta$, show that this quantity can be decomposed into contributions of the subclusters given in the table. The noble-gas atoms seem, as in NGMI Fe^0, to contribute additively to the noble-gas effect on the isomer shift of NGMI $FeCl_2$. The neon atoms around Fe and Cl have an opposite effect on the isomer shift, which leads to a partial cancellation of the noble-gas effect. As expected, the noble-gas influence decreases with distance. For NGMI $FeCl_2$, with Fe substituting a site in solid Ne and the molecular axis of $FeCl_2$ parallel to one of the crystal axes, the four nearest Ne neighbors of Fe at 3.2 Å in the plane through iron perpendicular to the molecular axis have a negligible effect on the Mössbauer parameters. The two axial Ne atoms yield $\Delta\delta = -0.05$ mm s^{-1}, and constitute the main contribution to the value obtained in the $FeCl_2$-Ne_6 cluster. Combining these values with the contributions of the four Ne neighbors around each of the two Cl atoms in the planes perpendicular to the molecular axis (i.e., two times -0.03 mm s^{-1}) leads to a total $\Delta\delta$ value of -0.11 mm s^{-1}. The Cl-Ne distance (2.26 Å) occurring for the "substituted" $FeCl_2$ is considerably below the sum of the van der Waals radius of Ne and the ionic radius of Cl^-, and is therefore probably smaller than the separations in real clusters. Larger Ne-Cl distances reduce the matrix effect $\Delta\delta = -0.11$ mm s^{-1}. We thus obtain for NGMI $FeCl_2$, in comparison with NGMI Fe^0, only a small matrix effect on the isomer shift. Two reasons for the reduction of the matrix effect on δ in NGMI $FeCl_2$ are (i) the small occupation number of the iron 4*s* orbital in $FeCl_2$ and (ii) the different sign of the various contributions to $\Delta\delta$, dependent on the Ne positions around $FeCl_2$. Concerning the results for ΔE_Q, we remark that, due to the strong directionality of the perturbation on $FeCl_2$ in the calculations with two nonaxial Ne atoms, the main component of the EFG becomes perpendicular to the molecular axis. In the remaining conformations the main component is along the molecular axis, as in the free molecule. In all cluster calculations presented in Table V, the component of the EFG along the molecular axis is reduced by the matrix effect.

CONCLUSIONS

(i) For the three modified Huzinaga basis sets, the UHF ground configuration of $FeCl_2$ and $FeBr_2$ is $^5\Delta$. The subsequent electron-correlation calculations at the MP4 level in $FeCl_2$ leave $^5\Delta$ lowest in energy. The STO-3G and STO-3G* basis sets are less appropriate for the description of the electronic structure in the two iron dihalides.

(ii) The one-electron ionization energies obtained by subtraction of UHF ground- and ionized-configuration energies are in better agreement with the experimental values than those obtained from molecular-orbital energies. Additional geometry optimizations in the ionized states further reduce the gap between the calculated and experimental ionization energies.

(iii) The calculated isomer shifts of free $FeCl_2$ and $FeBr_2$ relative to free Fe^0 are about 0.5 mm s^{-1} smaller than the values observed in NGMI experiments. The noble-gas effects on Fe^0 turn out to be non-negligible, viz., $\Delta\delta = \delta(\text{NGMI Fe}^0) - \delta(\text{free Fe}^0) \approx -0.4$ mm s^{-1}, while those on $FeCl_2$ are negligible. The calculated isomer shifts of NGMI $FeCl_2$ and $FeBr_2$ relative to NGMI Fe^0 are in reasonable agreement with the experimental values. The effect of the noble-gas atoms on the isomer shift in NGMI Fe is a nearly linear function of the 4*s* orbital occupation, and can be decomposed additively into contributions calculated in subclusters. The same kind of additivity is found for NGMI $FeCl_2$.

(iv) The experimental quadrupole splittings of the two NGMI iron dihalides lie in the range of the values evaluated in the $^5\Delta$ state. The calculations for $FeCl_2$ show a similar Fe—Cl distance dependence of the quadrupole splitting as reported in Ref. 3. However, in contrast with Ref. 3, our value for the EFG remains positive at the experimental Fe-Cl separation. The calculated value of ΔE_Q is affected by the choice of the basis set, contributions of electron correlation and the influence of the noble-gas atoms. The latter three effects on ΔE_Q are small in magnitude, but significant on a relative scale. For the above mentioned reasons, it is difficult to make a reliable theoretical prediction of the quadrupole splittings in NGMI dihalides.

ACKNOWLEDGMENT

One of us (J.G.) wishes to express his gratitude to the Alexander von Humboldt foundation for financial support.

[1]T. K. McNab, D. H. W. Carstens, D. M. Gruen, and R. L. McBeth, Chem. Phys. Lett. **13**, 600 (1972).
[2]F. J. Litterst, A. Schichl, and G. M. Kalvius, Chem. Phys. **28**, 89 (1978).
[3]D. E. Ellis, D. Guenzburger, and H. B. Jansen, Phys. Rev. B **28**, 3697 (1983).
[4]K. J. Duff, K. C. Mishra, and T. P. Das, Phys. Rev. Lett. **46**, 1611 (1981).
[5]C. W. DeKock and D. M. Gruen, J. Chem. Phys. **44**, 4387 (1966).
[6]G. E. Leroi, T. C. James, J. T. Hougen, and W. Klemperer, J. Chem. Phys. **36**, 2879 (1962).
[7]C. W. DeKock and D. M. Gruen, J. Chem. Phys. **49**, 4521 (1968).

[8]J. Berkowitz, D. G. Streets, and A. Garritz, J. Chem. Phys. **70**, 1305 (1979).
[9]E. Vajda, J. Tremmel, and I. Hargittai, J. Mol. Struct. **44**, 101 (1978).
[10]R. A. Frey, R. D. Werder, and H. H. Günthard, J. Mol. Spectrosc. **35**, 260 (1970).
[11]S. Lauer, V. R. Marathe, and A. X. Trautwein, Phys. Rev. A **19**, 1852 (1979).
[12]T. K. McNab, H. Micklitz, and P. H. Barrett, Phys. Rev. B **4**, 3787 (1971).
[13]M. Pasternak, Hyperfine Interact. **27**, 173 (1986).
[14]M. Braga, A. R. Riego, and J. Danon, Phys. Rev. B **22**, 5128 (1980).
[15]E. L. Bominaar, J. Guillin, V. R. Marathe, A. Sawaryn, and A. X. Trautwein, Hyperfine Interact. **40**, 111 (1988).
[16]P. F. Walch and D. E. Ellis, Phys. Rev. B **7**, 903 (1973).
[17]H. Shechter, J. G. Dash, M. Mor, R. Ingalls, and S. Bukshpan, Phys. Rev. B **14**, 1876 (1976).
[18]M. Frisch, J. S. Binkley, H. B. Schlegel, K. Raghavachari, R. Martin, J. J. P. Stewart, F. Bobrowicz, D. DeFrees, R. Seeger, R. Whiteside, D. Fox, E. Fluder, and J. A. Pople, GAUSSIAN86, Release C (Carnegie Mellon University, Pittsburgh, 1987).
[19]J. A. Pople and R. K. Nesbet, J. Chem. Phys. **22**, 571 (1959).
[20]C. Møller and M. S. Plesset, Phys. Rev. **46**, 618 (1934).
[21]V. R. Marathe, A. Sawaryn, A. X. Trautwein, M. Dolg, G. Igel-Mann, and H. Stoll, Hyperfine Interact. **36**, 39 (1987).
[22]R. Reschke, A. X. Trautwein, and J. P. Desclaux, J. Phys. Chem. Solids **38**, 837 (1977).
[23]V. R. Marathe and A. X. Trautwein, in *Advances in Mössbauer Spectroscopy,* edited by B. V. Thosar and P. K. Iyengar (Elsevier, Amsterdam, 1983), p. 398.
[24]V. R. Marathe, A. Sawaryn, and A. X. Trautwein, in *PDMS and Clusters Proceedings Wangerooge,* edited by E. R. Hilf, F. Kammer, and K. Wien (Springer-Verlag, Berlin, 1986), p. 182.
[25]S. Huzinaga, J. Andzelm, M. Klobukowski, E. Radzio-Andzelm, Y. Sakai, and H. Tatewaki, in *Gaussian Basis Sets for Molecular Calculations,* edited by S. Huzinaga (Elsevier, Amsterdam, 1984).
[26]T. C. Koopmans, Physica **1**, 104 (1933).
[27]J. C. Slater, in *The Self-Consistent Field for Molecules and Solids* (McGraw-Hill, New York, 1974), Vol. 4.
[28]M. Grodzicki, V. Männing, A. X. Trautwein, and J. M. Friedt, J. Phys. B **20**, 5595 (1987).
[29]S. Vajda, G. D. Sprouse, M. H. Rafailovich, and J. W. Noe, Phys. Rev. Lett. **47**, 1230 (1981).
[30]R. Montiel-Montoya, E. Bill, U. Gonser, S. Lauer, A. X. Trautwein, M. Schappacher, L. Ricard, and R. Weiss, in *The Coordination Chemistry of Metalloenzymes,* edited by I. Bertini, R. S. Drago, and C. Luchinat (Reidel, Dordrecht, 1983), p. 363.
[31]E. Bill, A. Gismelseed, D. Laroque, A. X. Trautwein, H. Nasri, J. Fischer, and R. Weiss, Hyperfine Interact. **42**, 881 (1988).
[32]H. Purdum, P. A. Montano, G. K. Shenoy, and T. Morrison, Phys. Rev. B **25**, 4412 (1982).
[33]P. A. Montano and G. K. Shenoy, Solid State Commun. **35**, 53 (1980).